

## A simple electronic circuit demonstrating Hopf bifurcation for an advanced undergraduate laboratory

Ishan Deo and Krishnacharya Khare

Citation: [American Journal of Physics](#) **90**, 908 (2022); doi: 10.1119/5.0062969

View online: <https://doi.org/10.1119/5.0062969>

View Table of Contents: <https://aapt.scitation.org/toc/ajp/90/12>

Published by the [American Association of Physics Teachers](#)

---

### ARTICLES YOU MAY BE INTERESTED IN

#### [Approximate insightful ODE solutions](#)

[American Journal of Physics](#) **90**, 887 (2022); <https://doi.org/10.1119/5.0131531>

#### [Charging a supercapacitor through a lamp: A power-law RC decay](#)

[American Journal of Physics](#) **90**, 895 (2022); <https://doi.org/10.1119/5.0065500>

#### [Exploration of the Q factor for a parallel RLC circuit](#)

[American Journal of Physics](#) **90**, 903 (2022); <https://doi.org/10.1119/5.0074843>

#### [Graphical analysis of an oscillator with constant magnitude sliding friction](#)

[American Journal of Physics](#) **90**, 889 (2022); <https://doi.org/10.1119/5.0073812>

#### [Chinese Abstracts](#)

[Chinese Journal of Chemical Physics](#) **35**, i (2022); <https://doi.org/10.1063/1674-0068/35/05/cabs>

#### [The size of the Sun](#)

[American Journal of Physics](#) **90**, 914 (2022); <https://doi.org/10.1119/5.0081964>

---



# A simple electronic circuit demonstrating Hopf bifurcation for an advanced undergraduate laboratory

Ishan Deo<sup>a)</sup> and Krishnacharya Khare<sup>b)</sup>

*Department of Physics, Indian Institute of Technology Kanpur, Kanpur 208016, India*

(Received 10 July 2021; accepted 26 September 2022)

A nonlinear electronic circuit comprising of three nodes with a feedback loop is analyzed. The system has two stable states, a uniform state and a sinusoidal oscillating state, and it transitions from one to another by means of a Hopf bifurcation. The stability of this system is analyzed with nonlinear equations derived from a repressilator-like transistor circuit. The apparatus is simple and inexpensive, and the experiment demonstrates aspects of nonlinear dynamical systems in an advanced undergraduate laboratory setting. © 2022 Published under an exclusive license by American Association of Physics Teachers.

<https://doi.org/10.1119/5.0062969>

## I. INTRODUCTION

A simple electronic circuit with a nonlinear electronic component can exhibit chaotic behavior.<sup>1–3</sup> Mishina *et al.* used a simple analog electronic circuit and demonstrated successive bifurcations leading to chaotic regimes.<sup>4</sup> Later Hellen used a slightly improved electronic circuit based on a simple nonlinear system, a finite difference equation with a quadratic return map, and showed bifurcation diagrams on an oscilloscope.<sup>5</sup> Goswami and Ray used a simple electronic circuit with a voltage-controlled current source, which exhibits feature-rich dynamics and several bifurcations.<sup>6</sup> Sack *et al.* constructed an electronic circuit which possessed remarkable organization in periodic oscillations in parameter space.<sup>7</sup> Cabeza *et al.* developed an electronic circuit with broad cycles.<sup>8</sup> Even an electronic circuit with a single transistor can display nonlinear behavior like limit cycles such as in the Hartley and Colpitts oscillators.<sup>9</sup>

The Hopf bifurcation is a special kind of bifurcation that involves the transition from stable behaviour of a system to periodic and vice versa.<sup>1</sup> It is prevalent in many physical phenomena, including repressilators in genetic networks, inverted pendulums, fluid flow about a sphere, and electronic circuits with negative differential resistance components.<sup>10–14</sup> Particularly, it is from the repressilator-based configuration that we get our motivation for the circuit. A repressilator is a genetic regulatory network comprised of at least one feedback loop of at least three genes. Taking inspiration from this, Rim *et al.* constructed an electronic circuit with a negative feedback loop consisting of three nodes, where each node models a gene.<sup>15</sup> The primary component of each node is a transistor, which serves as the means for negative feedback between nodes. We present a detailed analysis of the dynamics of the Hopf bifurcation in this 3-node electronic circuit. We obtain explicit formulae for the dependence of the bifurcation resistance on the applied voltage and for the variation of the fixed point voltage with resistance and applied voltage. The transistors used here are inexpensive, and the other components are easily found in any undergraduate physics laboratory. The theory of the Hopf bifurcation is also relatively simple, requiring only knowledge of multivariable calculus and calculus-based classical mechanics. Coupled with the simplicity of the circuit design and the circuit analysis, this experiment is appropriate to introduce advanced

undergraduate students to the fascinating world of nonlinear dynamics.

## II. STRUCTURE OF THE CIRCUIT

The electronic circuit we use here has been taken from the paper by Rim *et al.*<sup>15</sup> It consists of three identical nodes, which are connected to each other in a cycle to form a negative feedback loop. The structure of each node is shown in Fig. 1, where the transistor, resistors  $R_1$  and  $R_2$ , and the capacitor all have fixed values. The resistor  $R_3$  is variable and is the independent bifurcation parameter of the system. The transistor used in a node is an NPN bipolar junction transistor (BJT) with  $V_B$ ,  $V_C$ , and  $V_E$  as base, collector, and emitter voltages, respectively, and  $I_B$ ,  $I_C$ , and  $I_E$  as corresponding currents.  $V_i$ ,  $I_i$ ,  $V_o$ , and  $I_o$  represent input and output voltages and currents, respectively, and  $V_{CC}$  is the supply voltage. In the analysis, all the time-dependent parameters are written in corresponding lower case letters. The entire circuit comprising all the three nodes is shown in Fig. 2. So, the cycle is formed by:

- The  $v_o$  of the first node serving as the  $v_i$  of the second node;
- The  $v_o$  of the second node serving as the  $v_i$  of the third node;
- The  $v_o$  of the third node serving as the  $v_i$  of the first node.

In the whole loop, each of the three resistances labelled  $R_3$  have the same values at all times and are varied simultaneously.

## III. CIRCUIT ANALYSIS

### A. Modelling of an NPN BJT in active mode

An NPN BJT has four modes of operation: active, cutoff, reverse active, and saturation, which depend on whether  $v_{BE} = v_B - v_E$  and  $v_{CB} = v_C - v_B$  are positive or negative, where  $v_{BE}$  and  $v_{CB}$  are the transient voltages at the base-emitter and collector-base junctions, respectively. In our experimental setup, BJT is in the active mode (that is, both  $v_{BE}$  and  $v_{CB}$  are positive). So, we focus on this mode only here. For an NPN BJT in the active mode, the Ebers-Moll model gives, under the assumption of physically realistic voltages, the equations

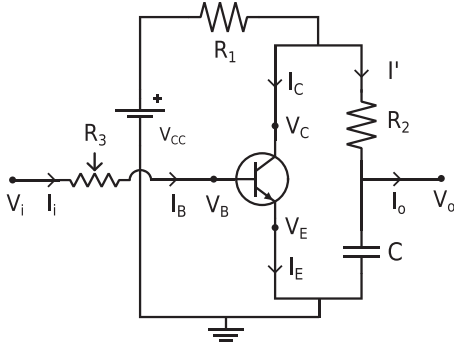


Fig. 1. Circuit diagram of one node showing the components and parameters.  $R_3$  is the variable input resistor, which is also used as the feedback resistor when different nodes are connected together.

$$i_C = I_S \exp \frac{v_{BE}}{V_T}, \quad (1)$$

$$i_C = \alpha i_E, \quad (2)$$

$$i_C = \beta i_B. \quad (3)$$

Here,  $I_S$  is the saturation current,  $V_T$  is the thermal voltage, and  $\alpha$  and  $\beta$  are two proportionality constants. Now, we also have  $i_E = i_C + i_B$ , with all three positive (as  $v_{BE}$  and  $v_{CB}$  are positive). Thus, we get the relations  $\alpha = \beta/(1 + \beta)$  or  $\beta = \alpha/(1 - \alpha)$  between  $\alpha$  and  $\beta$ . For typical NPN BJTs,  $\beta$  ranges from 50 to 200, and so  $\alpha$  ranges from 0.98 to 0.99. Also,  $I_S$  is of the order of  $10^{-12}$  A for typical NPN BJTs, and  $V_T = 0.025875$  V at room temperature (298 K). For further details on NPN BJTs, readers are encouraged to refer to Ref. 9.

### B. Lambert W function

The Lambert  $W$  function  $W(x)$  is defined as the real solution of the equation  $ye^y = x$ . We summarize here some properties of this function for positive  $x$ , which will be used throughout. For detailed proofs, one may look at Ref. 17.

- **Single-valued:** The function  $W(x)$  is single valued, that is, for any  $x$ , there is only one real  $y$  such that  $ye^y = x$ .
- **Positive:** For  $x > 0$ ,  $W(x) > 0$ .
- **Monotonic:**  $W(x)$  is a monotonically increasing function. That is  $x_1 > x_2 \Rightarrow W(x_1) > W(x_2)$ .

### • Derivative:

$$\frac{dW(x)}{dx} = \frac{1}{x} \frac{W(x)}{1 + W(x)}. \quad (4)$$

### C. Modelling the node

For this circuit, as the emitter is grounded in the node,  $v_E = 0$ , and so  $v_B = v_{BE}$ . Applying Kirchoff's Laws and the results in Sec. III A, we get

$$\frac{dv_o}{dt} = \frac{V_{CC} - v_o - i_C R_1 - i_o (R_1 + R_2)}{C(R_1 + R_2)}, \quad (5)$$

$$\log \frac{i_C}{I_S} = \frac{v_i}{V_T} - \frac{R_3}{\beta V_T} i_C. \quad (6)$$

Let us take  $a = I_S R_3 / \beta V_T$  for simplicity. Then, we can solve for  $i_C$  with the help of the Lambert  $W$  function  $W(x)$ ,

$$i_C = \frac{\beta V_T}{R_3} W \left( a \exp \frac{v_i}{V_T} \right). \quad (7)$$

Note that  $a$  depends only on  $R_3$  (the bifurcation parameter). On substituting this in Eq. (5), we get the variation of  $v_o$  as

$$\frac{dv_o}{dt} = \frac{V_{CC} - v_o - \beta V_T \frac{R_1}{R_3} W \left( a \exp \frac{v_i}{V_T} \right) - i_o (R_1 + R_2)}{C(R_1 + R_2)}. \quad (8)$$

### D. Modelling the circuit

For this circuit, the input of a node is the output of the previous node. So, the values of  $V$  and  $I$  of a node depend on both the preceding and succeeding nodes. Now, formally, let us define node 4 to be identical to node 1, and node 0 as identical to node 3. Then, we can say that node  $n$  depends on the nodes  $n - 1$  and  $n + 1$ . Thus, we get for current

$$i_{C_n} = \frac{\beta V_T}{R_3} W \left( a \exp \frac{v_{n-1}}{V_T} \right), \quad (9)$$

$$i_n = i_{B_{n+1}}, \quad (10)$$

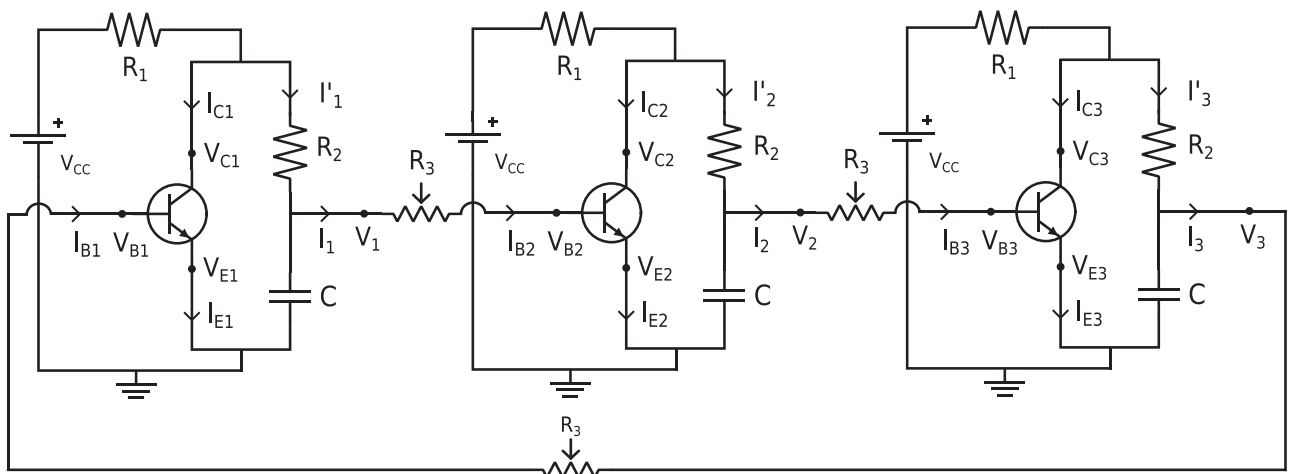


Fig. 2. Circuit diagram of the complete circuit having three nodes and feedback loop.

$$= \frac{V_T}{R_3} W\left(a \exp \frac{v_n}{V_T}\right), \quad (11)$$

and, hence, for voltage

$$\begin{aligned} \frac{dv_n}{dt} &= \frac{V_{CC} - v_n}{C(R_1 + R_2)} - \frac{V_T}{CR_3} \\ &\times \left[ W\left(a \exp \frac{v_n}{V_T}\right) + \beta \frac{R_1}{R_1 + R_2} W\left(a \exp \frac{v_{n-1}}{V_T}\right) \right]. \end{aligned} \quad (12)$$

#### IV. MATHEMATICAL ANALYSIS OF THE MODEL

Due to the nonlinearity, we are unable to find a closed form solution for this system. Instead, we analyze the behaviour of the stable states of the system.

##### A. Fixed point

The system has a fixed point when  $dv_n/dt = 0$  for  $n = 1, 2, 3, 12$ . That is

$$\begin{aligned} V_{CC} &= v_1 + V_T \left[ \frac{R_1 + R_2}{R_3} W\left(a \exp \frac{v_1}{V_T}\right) \right. \\ &\quad \left. + \beta \frac{R_1}{R_3} W\left(a \exp \frac{v_3}{V_T}\right) \right]; \end{aligned} \quad (13)$$

$$\begin{aligned} V_{CC} &= v_2 + V_T \left[ \frac{R_1 + R_2}{R_3} W\left(a \exp \frac{v_2}{V_T}\right) \right. \\ &\quad \left. + \beta \frac{R_1}{R_3} W\left(a \exp \frac{v_1}{V_T}\right) \right]; \end{aligned} \quad (14)$$

$$\begin{aligned} V_{CC} &= v_3 + V_T \left[ \frac{R_1 + R_2}{R_3} W\left(a \exp \frac{v_3}{V_T}\right) \right. \\ &\quad \left. + \beta \frac{R_1}{R_3} W\left(a \exp \frac{v_2}{V_T}\right) \right]. \end{aligned} \quad (15)$$

##### 1. Equality of $n$ at fixed point

Without loss of generality, we can assume that  $v_1 \leq v_2 \leq v_3$  at the fixed point. Subtracting Eq. (14) from Eq. (15), we get

$$\begin{aligned} (v_3 - v_2) + V_T \frac{R_1 + R_2}{R_3} \left[ W\left(a \exp \frac{v_3}{V_T}\right) - W\left(a \exp \frac{v_2}{V_T}\right) \right] \\ = V_T \beta \frac{R_1}{R_3} \left[ W\left(a \exp \frac{v_1}{V_T}\right) - W\left(a \exp \frac{v_2}{V_T}\right) \right]. \end{aligned} \quad (16)$$

The function  $W(x)$  is monotonic for positive arguments. So, as  $v_3 \geq v_2$  by assumption, the left hand side of the equation is  $\geq 0$ . Yet, as  $v_1 \leq v_2$ , the right hand side of the equation is  $\leq 0$ . Thus, the two sides are equal only when  $v_1 = v_2 = v_3 \equiv v_P$ . Hence, any fixed point of the system must be of the form  $(v_P, v_P, v_P)$ .

##### 2. Existence of unique fixed point

At a fixed point  $(v_P, v_P, v_P)$ , the equation of the system is

$$V_{CC} = v_P + V_T \frac{R_1(1 + \beta) + R_2}{R_3} W\left(a \exp \frac{v_P}{V_T}\right). \quad (17)$$

Let  $R = R_1(1 + \beta) + R_2$  and  $R' = R + R_3$  for simplicity. Then, we can solve for  $v_P$  to get

$$v_P = V_{CC} - V_T \frac{R}{R'} W\left(\frac{I_S R'}{\beta V_T} \exp \frac{V_{CC}}{V_T}\right). \quad (18)$$

Thus, there exists a fixed point, and as  $W(x)$  is single-valued, it is unique. Let us also derive a useful equation for future use. Defining  $y = (I_S R' / \beta V_T) \exp(V_{CC} / V_T)$  for ease of notation, we have

$$W\left(a \exp \frac{v_P}{V_T}\right) = \frac{R_3}{R'} W(y). \quad (19)$$

##### B. Jacobian and its Eigenvalues

In order to determine whether the system has a Hopf bifurcation, we need to determine the eigenvalues of the Jacobian. The Jacobian of the system has two terms

$$A = \left( \frac{\partial}{\partial v_n} \frac{dv_n}{dt} \right) \Big|_P \quad (20)$$

$$= -\frac{1}{C} \left( \frac{1}{R_1 + R_2} + \frac{W(y)}{R' + R_3 W(y)} \right), \quad (21)$$

$$B = \left( \frac{\partial}{\partial v_{n-1}} \frac{dv_n}{dt} \right) \Big|_P \quad (22)$$

$$= -\frac{\beta R_1}{C R_1 + R_2 R' + R_3 W(y)}. \quad (23)$$

In terms of these parameters, the Jacobian is

$$J = \begin{bmatrix} A & 0 & B \\ B & A & 0 \\ 0 & B & A \end{bmatrix}. \quad (24)$$

This matrix has the eigenvalues

$$\lambda_1 = A - \frac{B}{2} + \frac{\sqrt{3}}{2} Bi, \quad (25)$$

$$\lambda_2 = A - \frac{B}{2} - \frac{\sqrt{3}}{2} Bi, \quad (26)$$

$$\lambda_3 = A + B. \quad (27)$$

As  $A$  and  $B$  are real, we have a pair of complex eigenvalues.

##### C. Existence of Hopf bifurcation

The mathematics behind Hopf bifurcations is well described in textbooks.<sup>1,16</sup> Interested readers can refer them to learn about the existing result of the Hopf bifurcation and its proof. In terms of the system we are analyzing, the existing result translates to the following. The circuit displays a Hopf bifurcation if it has a fixed point of the node voltage  $(v_P, v_P, v_P)$ , and at this fixed point, there



exists a critical value  $R_c$  of the bifurcation parameter  $R_3$  at which the eigenvalues of the Jacobian satisfy the following properties:

$$\operatorname{Re}(\lambda_1) = \operatorname{Re}(\lambda_2) = 0 \quad \text{and} \quad \operatorname{Re}(\lambda_3) \neq 0, \quad (28)$$

$$\frac{d}{dR_3}(\operatorname{Re}(\lambda_1)) = \frac{d}{dR_3}(\operatorname{Re}(\lambda_2)) \neq 0. \quad (29)$$

As we saw in Subsection IV A, the system does indeed have a fixed point. Also, as  $A, B$  are negative,  $\lambda_3 = A + B \neq 0$ , which satisfies part of the first condition. For the rest, it is evident that the existence of Hopf bifurcation depends on

$$A - \frac{B}{2} = -\frac{1}{C(R_1 + R_2)} \left[ 1 + \left( R_1 + R_2 - \frac{\beta R_1}{2} \right) \times \frac{W(y)}{R' + R_3 W(y)} \right]. \quad (30)$$

Let us check the second condition first. Computing the derivative, we get

$$\frac{d}{dR_3} \left( A - \frac{B}{2} \right) = \frac{R_1 + R_2 - \frac{\beta R_1}{2}}{C(R_1 + R_2)} \frac{W(y)^2}{(R' + R_3 W(y))^2} \times \frac{2 + W(y)}{1 + W(y)}. \quad (31)$$

As  $W(x) > 0$  for  $x > 0$ , this derivative is non-zero for all values of  $R_3$ —that is, the second condition holds for any  $R_3$ . For the first condition, let us define  $R_0 = \beta R_1 / 2 - R_1 - R_2 - R_3$ . Then,  $A = B/2$  implies

$$W(y) = \frac{R'}{R_0} = \frac{3\beta R_1}{2R_0} - 1. \quad (32)$$

After some algebraic manipulations, this becomes

$$R_3 = \frac{\beta R_1}{2} \left( 1 - \frac{3}{W \left( \frac{3I_S R_1}{2V_T} \exp \frac{V_{CC} + V_T}{V_T} \right)} \right) - R_1 - R_2. \quad (33)$$

Thus, we get a critical value of  $R_3$ , and hence, the system displays a Hopf bifurcation. For future use, the above equation can be inverted to get  $V_{CC}$

$$\frac{V_{CC}}{V_T} = \frac{3}{1 - \frac{2R_3 + R_1 + R_2}{\beta R_1}} + \log \frac{\frac{2V_T}{I_S R_1}}{1 - \frac{2R_3 + R_1 + R_2}{\beta R_1}} - 1. \quad (34)$$

From this, as  $W(x) > 0$  for  $x > 0$ , we also get the inequality

$$\beta > 2 \frac{R_3 + R_1 + R_2}{R_1}. \quad (35)$$

Thus, this inequality holds if and only if the system displays a Hopf bifurcation at that value of  $R_3$  (Fig. 3).

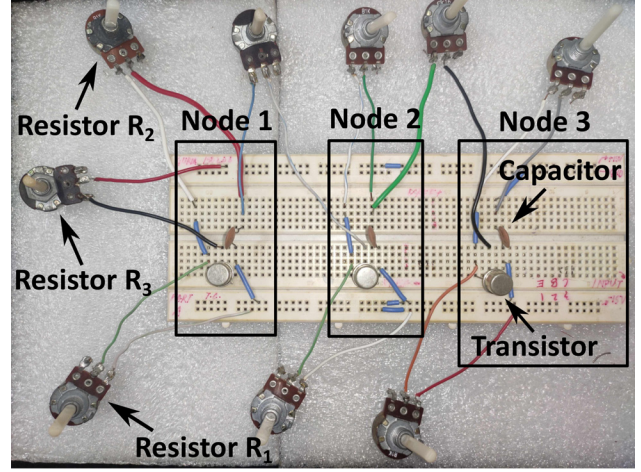


Fig. 3. Photograph of the actual circuit prepared on a breadboard showing all three nodes with electronic components.

## V. EXPERIMENTAL SETUP

We constructed the circuit as shown in Fig. 2 with the following circuit components:

- $R_1$ :  $1k\Omega$  potentiometer
- $R_2$ :  $1k\Omega$  potentiometer
- $R_3$ :  $100k\Omega$  potentiometer
- $C$ :  $220$  nF capacitor
- Transistor (NPN) model: SL100

Note that even though the resistance values  $R_1$  and  $R_2$  are held constant during the experiment, we have used potentiometers for them. This is to ensure that the values of  $R_1$  and  $R_2$  are exactly  $1k\Omega$  and, thus, reduce the error in the voltages measured. We used an ordinary lab digital storage oscilloscope (DSO) to measure the voltages  $v_i$  of the capacitor as a function of the different values of resistance  $R_3$  and applied voltage  $V_{CC}$ . As it was easier to change  $V_{CC}$  as compared to  $R_3$ , we measured  $v_i$  on varying  $V_{CC}$  at a fixed  $R_3$ , for multiple values of  $R_3$ .

## VI. RESULTS AND DISCUSSIONS

### A. Preliminary results

#### 1. Verification of active mode of transistors

In each measurement, for each transistor, the voltage  $v_{BE}$  was around  $0.65 - 0.75$  V, while the voltage  $v_{CB}$  was positive. So, the transistor is indeed operating in the active mode.

#### 2. $\beta$ value of transistors

The  $\beta$  value of the transistor of each node is given in Table I. These values are not equal, possibly due to manufacturing defects. Thus, we use the mean value of  $\beta = 130.5$ .

Table I.  $\beta$  values of transistors of the circuit.

Node 1	Node 2	Node 3	Mean	Standard deviation	% Error
129.6	131.7	130.2	130.5	1.08	0.83

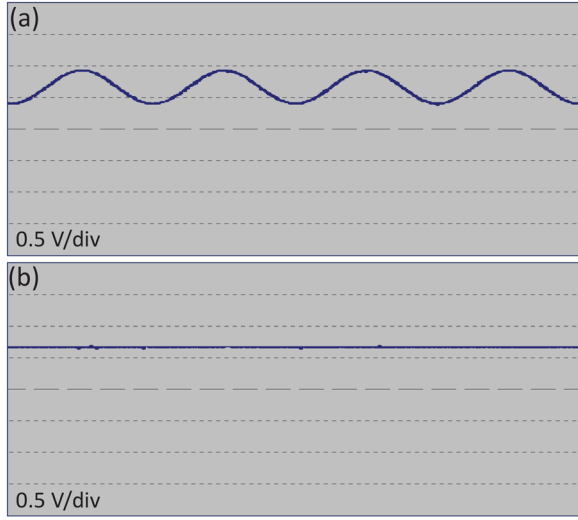


Fig. 4. Hopf bifurcation at node 2 for a bifurcation resistance  $R_3 = 61.0k\Omega$  by varying  $V_{CC}$ . Waveforms in a digital oscilloscope at (a) voltage before the Hopf bifurcation and (b) afterwards.

### B. Existence of Hopf bifurcation and variation with applied voltage

On fixing a value of  $R_3$ , we varied  $V_{CC}$  applied to the circuit, in order to find its value at which we have a Hopf bifurcation. Figure 4 shows the Hopf bifurcation on a digital oscilloscope at node 2 of the circuit by varying  $V_{CC}$  with  $R_3 = 61.0k\Omega$ . The experimental values of  $R_3$  and  $V_{CC}$  are listed in the Table II. From the data, we can see that there is no Hopf bifurcation at  $R_3 = 64k\Omega$ , as we have

$$\begin{aligned} 2 \frac{R_3 + R_1 + R_2}{R_1} &= 2 \frac{64 \times 10^3 + 10^3 + 10^3}{10^3} \\ &= 132 > \beta = 130.5, \end{aligned} \quad (36)$$

which satisfies the condition of inequality (Eq. (35)). For smaller values of  $R_3$ , Hopf bifurcation occurs. In Fig. 5, we have plotted these values and compared them to the theoretical curve. In Fig. 5, we see that the experimental data closely matches with the theoretical curve constructed using Eq. (34). This supports the theoretical result we had derived previously.

### C. Type of Hopf bifurcation

There are two types of Hopf bifurcations: supercritical and subcritical. The most important difference between them, for us, is reversibility. That is, suppose we vary the bifurcation resistance  $R_3$  such that the bifurcation occurs and then go

Table II. Bifurcation resistance vs applied voltage variation.

Resistance at bifurcation ( $R_3$ ) ( $k\Omega$ )	Applied voltage ( $V_{CC}$ ) (V)
64.0	No bifurcation occurs
62.5	7.4
62.0	4.2
61.5	3.4
61.0	2.9
60.5	2.4

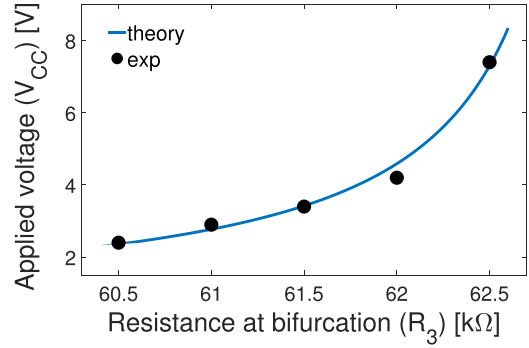


Fig. 5. Applied voltage ( $V_{CC}$ ) vs resistance at bifurcation ( $R_3$ ).  $R^2$  value of this plot is 0.9887.

back to the original value of  $R_3$ . Then, the system displaying supercritical Hopf bifurcation will revert back to the original voltage state, while it will not for a subcritical Hopf bifurcation. On performing this test to the circuit, we observed that for each value of applied voltage, the fixed-point node voltage returned to the original value. Thus, the circuit displays a supercritical Hopf bifurcation.

### D. Variation of fixed point voltage with applied voltage and resistance

In the fixed point regime of the circuit, we varied the resistance  $R_3$  and applied voltage  $V_{CC}$  and observed the values of  $v_P$  obtained at each node. From the readings, we can see that the voltages in each of the three nodes are not identical. This can be attributed to the three nodes being dissimilar, which occurs due to the transistors having different  $\beta$  values, for reasons mentioned before. We also plotted the variation of  $v_P$  with  $V_{CC}$  at a fixed resistance  $R_3$  and compared it with the theoretical curve (obtained from Eq. (18)) in Fig. 6. We can see that there is an excellent match between experimental data and theoretical results, thus supporting the results we have obtained.

## VII. CONCLUSION

In this paper, we present a simple electronic circuit consisting of three nodes and a feedback loop, which is similar to a genetic repressilator. The circuit undergoes a Hopf

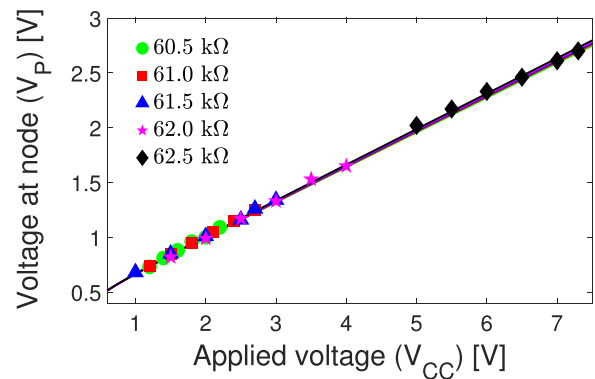


Fig. 6. Plots of fixed point voltage ( $V_P$ ) with applied voltage ( $V_{CC}$ ) for different bifurcation resistances ( $R_3$ ). The solid curve represents the theoretical result given in Eq. (18), while the data points represent the experimentally obtained values. The  $R^2$  values of all five graphs range from 0.9753 to 0.9935.

bifurcation based on various system parameters. DC analysis of the circuit tells us how the voltage (amplitude) varies with the resistance (bifurcation parameter) in the limit cycle close to the bifurcation point. Since all components of the apparatus involved are readily available, and prerequisite knowledge is within the level of a third year college education in physics, this experiment serves as a good introduction for students to experimental nonlinear dynamics.

## ACKNOWLEDGMENTS

This study was supported by the Modern Physics Laboratory of the Department of Physics, Indian Institute of Technology Kanpur and Science and Engineering Research Board (SERB) New Delhi (Project No. CRG/2019/000915). The authors thank Upendra Kumar Parashar for valuable help with the experiments.

## AUTHOR DECLARATIONS

### Conflict of Interest

The authors have no conflicts of interest to disclose.

<sup>a)</sup>ORCID: 0000-0003-4571-5707.

<sup>b)</sup>Electronic mail: kcharya@iitk.ac.in

<sup>1</sup>S. H. Strogatz, *Nonlinear Dynamics and Chaos: with Applications to Physics, Biology, Chemistry, and Engineering*, 2nd ed. (Westview Press, Boulder, CO, 2015), pp. 251–256.

<sup>2</sup>M. Heinrich, T. Dahms, V. Flunkert, S. W. Teitsworth, and E. Schöll, “Symmetry-breaking transitions in networks of nonlinear circuit elements,” *New J. Phys.* **12**, 113030 (2010).

<sup>3</sup>J. C. Sprott, “Simple chaotic systems and circuits,” *Am. J. Phys.* **68**, 758–763 (2000).

<sup>4</sup>T. Mishina, T. Kohmoto, and T. Hashi, “Simple electronic circuit for the demonstration of chaotic phenomena,” *Am. J. Phys.* **53**, 332–334 (1985).

<sup>5</sup>E. H. Hellen, “Real-time finite difference bifurcation diagrams from analog electronic circuits,” *Am. J. Phys.* **72**, 499–502 (2004).

<sup>6</sup>D. Goswami and S. Ray, “Feature-rich bifurcations in a simple electronic circuit,” e-print [arXiv:1705.07101v1](https://arxiv.org/abs/1705.07101v1).

<sup>7</sup>A. Sack, J. G. Freire, E. Lindberg, T. Pöschel, and J. A. C. Gallas, “Discontinuous spirals of stable periodic oscillations,” *Sci. Rep.* **3**, 3350 (2013).

<sup>8</sup>C. Cabeza, C. A. Briozzo, R. Garcia, J. G. Freire, and J. A. C. Gallas, “Periodicity hubs and wide spirals in a two-component autonomous electronic circuit,” *Chaos, Solitons Fractals* **52**, 59–65 (2013).

<sup>9</sup>A. S. Sedra and K. C. Smith, *Microelectronic Circuits*, 5th ed. (Oxford U. P., New York, 2004).

<sup>10</sup>A. Verdugo, “Hopf bifurcation analysis of the repressilator model,” *Am. J. Comput. Math.* **8**, 137–152 (2018).

<sup>11</sup>James A. Blackburn, H. J. T. Smith, and N. Grønbech-Jensen, “Stability and Hopf bifurcations in an inverted pendulum,” *Am. J. Phys.* **60**, 903–908 (1992).

<sup>12</sup>J. P. Sharpe and N. Sungar, “Supercritical bifurcation in a simple mechanical system: An undergraduate experiment,” *Am. J. Phys.* **78**(5), 520–523 (2010).

<sup>13</sup>P. G. Drazin and W. H. Reid, *Hydrodynamic Stability*, 2nd ed. (Cambridge U. P., England, 2004), p. 405.

<sup>14</sup>C. R. Wallis and S. W. Teitsworth, “Hopf bifurcations and hysteresis in resonant tunneling diode circuits,” *J. Appl. Phys.* **76**, 4443–4445 (1994).

<sup>15</sup>D. N. Rim, P. Cremades, and P. Kaluza, “A simple electronic device to experiment with the Hopf bifurcation,” *Rev. Mex. Fís.* **E 65**, 58–63 (2019).

<sup>16</sup>J. Guckenheimer and P. Holmes, *Nonlinear Oscillations Dynamical Systems, and Bifurcations of Vector Fields*, 1st ed. (Springer-Verlag, New York, 1983), pp. 151–152.

<sup>17</sup>S. M. Stewart, “A new elementary function for our curricula?,” *Aust. Senior Math. J.* **19**(2), 8–26 (2005).



### Thunder Houses

These three tiny thunder houses were in the demonstration apparatus collection of the University of Maine when I visited in 2011. In these examples, the spark from a Leiden jar travels down a wire to a spark gap that is near a small amount of explosive material (often dampened gunpowder) in the middle of the house. When this explodes, the top blows off, and we see the reason for installing lightning rods on a house. (Picture and text by Thomas B. Greenslade, Jr., Kenyon College)